TITLE PAGE

Citation Format:

L. Di Sieno, E. Avanzi, F. Acerbi, A. Gola, M. Lacerenza, A. Behera, D. Contini, A. Dalla Mora, "Breaking the rules of time-domain diffuse optics: working with 1 cm2 SiPM and well-beyond the single-photon statistics," Proc. SPIE 11974, Biomedical Applications of Light Scattering XII, 119740A (3 March 2022);

Copyright notice:

DOI abstract link:

10.1117/12.2608656

PROCEEDINGS OF SPIE

SPIEDigitalLibrary.org/conference-proceedings-of-spie

Breaking the rules of time-domain diffuse optics: working with 1 cm2 SiPM and well-beyond the single-photon statistics

L. Di Sieno, E. Avanzi, F. Acerbi, A. Gola, M. Lacerenza, et al.

L. Di Sieno, E. Avanzi, F. Acerbi, A. Gola, M. Lacerenza, A. Behera, D. Contini, A. Dalla Mora, "Breaking the rules of time-domain diffuse optics: working with 1 cm2 SiPM and well-beyond the single-photon statistics," Proc. SPIE 11974, Biomedical Applications of Light Scattering XII, 119740A (3 March 2022); doi: 10.1117/12.2608656

SPIE.

Event: SPIE BiOS, 2022, San Francisco, California, United States

Breaking the rules of time-domain diffuse optics: working with 1 cm^2 SiPM and well-beyond the single-photon statistics

L. Di Sieno*[a], E. Avanzi[a], F. Acerbi[b], A. Gola[b], M. Lacerenza[a],
A. Behera[a], D. Contini[a] and A. Dalla Mora[a]
[a]Politecnico di Milano, Dipartimento di Fisica, Piazza Leonardo da Vinci 32, 20133 Milano (Italy);
[b] Fondazione Bruno Kessler (FBK), Via Sommarive, 38123 Trento (Italy)

ABSTRACT

Time domain diffuse optics (TD-DO) relies on the injection of ps laser pulses and on the collection of the arrival times of scattered photons. To reach the ultimate limits of the technique (allowing to investigate even structures at depth >5 cm), a large area detector is needed. To this extent, we realized and present a new silicon photomultiplier featuring a 1 cm^2 area. To the best of our knowledge, it represents the largest detector ever proposed for TD-DO and shows a light harvesting capability which is more than 1 decade larger than the state-of-the-art technology system. To assess its suitability for TD-DO measurements, we tested the detector with several procedures from shared protocols (BIP, nEUROPt and MEDPHOT). However, the light harvesting capability of a detector with large area can be proficiently exploited only if coupled to timing electronics working in sustained count-rate CR (i.e., well above the single photon statistics). For this reason, we study the possibility to work in a regime where (even more than) one photon per laser pulse is detected (i.e., more than 100% laser repetition rate) exploiting in-silico technology. The results show that the possibility to use sustained count-rate represents a dramatic improvement in the number of photons detected with respect to current approaches (where count-rate of 1-5% of the laser repetition rate are used) without significant losses in the measurement accuracy. This represents a new horizon for TD-DO measurements, opening the way to new applications (e.g., optical investigation of the lung or monitoring of fast dynamics never studied before).

Keywords: single-photon detector; time-domain diffuse optics; turbid media; single-photon statistics

1. INTRODUCTION

Time domain diffuse optics (TD-DO) is a non-invasive technique which allows to sample diffusive media by injecting short pulses of laser light and recording the temporal distribution of re-emitted photons[1] (the so called distribution of time-of-flight, DTOF). Indeed, when travelling into a diffusive medium, photons can encounter two phenomena: absorption or scattering (measured through the absorption and reduced scattering coefficient, μ_a and μ_s' respectively). One of the main advantages of TD-DO technique is the capability to disentangle those contributions, which are related to different aspects of the medium: the absorption is connected to the chemical composition, while the reduced scattering depends on the structure of the sample. Another advantage of the TD-DO is the capability to encode the mean penetration depth in the arrival times of photons: indeed, the longer is the path of the photons inside the medium, the higher is the probability they reach deep structures[2]. However, it must be considered that TD-DO applications are "photon starved" and to push the technique to its physical limits, there is the need to improve the light harvesting capability[3].

To move towards this direction, the TD-DO field takes advantage of the last technological advancements for pulsed laser sources, single-photon detectors and timing electronics both in terms of performances as well as miniaturization and integration[4–6]. More in detail, in the last years Silicon PhotoMultipliers (SiPMs) have been introduced in diffuse optics thus allowing to merge the advantages of solid-state detectors (e.g., robustness, low susceptibility to electromagnetic interferences, possibility to be integrated etc.) with the large area, a typical advantage of bulky and fragile detectors such as PhotoMultipliers Tubes[7]. The increase in the active area of the detector up to few mm^2 (from 1 to 10 mm^2)[8–10] and the possibility to put it in contact with the sample (avoiding optical fibers) are, indeed, two of the requirements needed to exploit all the potentialities of the time-domain technique[3].

*laura.disieno@polimi.it; phone 0039 02 23996597

Biomedical Applications of Light Scattering XII, edited by Adam Wax, Vadim Backman,
Proc. of SPIE Vol. 11974, 119740A · © 2022 SPIE · 1605-7422 · doi: 10.1117/12.2608656

However, the large improvement in the light harvesting capability of the detector (i.e., the responsivity test defined in the Basic Instrumental Performance BIP protocol[11]) is not sufficient if not coupled to a high-throughput timing electronics. Indeed, the significant increase in the responsivity brings a larger number of detected photons that needs to be processed by the timing electronics. This improvement in the detected photons cannot be fully exploited if the single-photon statistics condition (i.e., rate of detected photons around 1-5% of the laser repetition rate[12]) has to be fulfilled.

To this extent, a new exploratory working regime has been tested. In Ref.[13], some of us demonstrated, in few cases, the possibility to successfully work with a throughput well beyond the single-photon statistics, provided that a suitable correction algorithm for pile-up distortion is applied[14].

In this work, we extensively present the largest-area detector for TD-DO applications with an active area of 1 cm^2 and a responsivity, which is more than 1 order of magnitude larger than other state-of-the-art microelectronic detectors suitable for TD-DO. We tested this detector using selected procedures from shared protocols for assessment of performance of diffuse optics instruments such as BIP, nEUROPt and MEDPHOT [11,15,16]. Once the use of the 1 cm^2 detector for diffuse optics was validated, an in-silico study has been performed to show that it is possible to work well above single-photon statistics without losing any information Moreover, this approach allows to achieve significant benefits such as improved visibility of an optical perturbation buried in depth (in case we increase the number of photons detected in the same integration time) or the decrease of the integration time (if the overall number of photons detected is fixed).

2. MATERIAL AND METHODS

2.1 Experimental setup

The experimental setup is similar to the one presented in Ref.[17]. Except for the responsivity test, we used a high-power pulsed diode laser with a laser-head emitting at 670 nm (PDL 828 "Sepia II" with LDH-P-670 Picoquant GmbH, Germany) which has a maximum average power up to 50 mW. Such a choice allows to exploit the large light harvesting capability of the detector. The laser light was attenuated by means of a variable optical attenuator and then injected into a step-index 600 μm diameter fiber. The other tip of the fiber was placed in contact with the sample. The photons re-emitted from the sample were then collected by the detector, which was put in contact with the sample to exploit the whole active area and numerical aperture.

The proposed detector is a cooled SiPM-based single-photon detection module (dimensions: 60 x 73 x 58 mm^3) exploiting a 10 x 10 mm^2 SiPM (NIR-HD technology with 50 μm cell pitch), which was specifically designed and then fabricated in FBK, Italy. Although the detector is a single chip, it is composed of 6 sub-SiPMs which are connected together externally in 2 groups and then merged to provide a single output signal. The detector is cooled at about -36°C using a 2-stage Peltier-cooler to keep the dark count rate (DCR) well below 1 Mcps. More detail on the electronics of the module as well as its basic characterization in terms of noise (DCR and correlated noise probability), photon detection efficiency as well as timing resolution (full-width at half-maximum FWHM as well as shape) can be found elsewhere[18].

Only for the responsivity test, we used the system described in Ref[19] since it allows to cover a broad spectral region ranging from 600 to 1100 nm.

Depending on the measurements, two kinds of phantoms were used: a liquid and a solid one. The former is a mixture of calibrated quantities[20] of water, intralipid (which gives the scattering properties) and black Indian ink (to give the absorption) to reach the optical properties of $\mu_a = 0.1\ cm^{-1}$ and $\mu_s' = 10\ cm^{-1}$ at 670 nm. Since the liquid phantom was employed to assess the maximum penetration depth of the system, we used an optical perturbation to be moved in depth. To this extent, we adopted a totally absorbing inclusion[21] (i.e., a cylinder made of black PVC) which induces an equivalent absorption perturbation of 0.17 cm^{-1} over 1 cm^3. The perturbation (aligned in the middle between source and detector) was moved in depth from 2.5 mm below the surface of the phantom up to 50 mm. For each position, 10 acquisition of 1 s each were recorded. Moreover, to sample the medium not affected by the presence of the perturbation, we moved it at a depth of 60 mm where its effect is negligible (the so-called homogeneous case).

On the other hand, to assess the light harvesting capability of the system (responsivity test of the BIP protocol) and to test its capability to properly recover the optical properties of homogeneous media (as dictated by the MEDPHOT protocols), we made use of solid phantoms. They are based on epoxy resin where TiO_2 and black toner were added, respectively, as scattering and absorbing particles. For MEDPHOT measurements we made use of a set of 32 phantoms whose reduced

scattering coefficients is labeled with four letters: A, B, C and D corresponding to 7, 11, 16, 20 cm^{-1} at 690 nm (conventionally true values). For each scattering value, 8 phantoms (labelled with numbers from 1 to 8) with an absorption coefficient of 0.01, 0.07, 0.14, 0.20, 0.27, 0.33, 0.38, 0.46 (conventionally true values at 690 nm) were employed. For more details on the responsivity phantom and on the MEDPHOT phantoms, readers can refer to the following publications[11,16].

All the experimental measurements have been conducted at "standard count-rate" (i.e., not exceeding significantly the single-photon statistics), being usually at about 1 Mcps above the DCR level.

2.2 BIP protocol

The BIP protocol was meant to assess the basic performances of the system for time-domain diffuse optics. Among the several tests needed to objectively assess the hardware performances of the setup without the sample, we adopted the responsivity one which evaluates the light harvesting capability of the system. As previously stated, the measurements were possible thanks to a dedicated phantom which mimics the Lambertian distribution of the light exiting from a diffusive media. Once the phantom calibration is known, it is possible to compute the responsivity value by measuring both the number of photons re-emitted from the phantom as well as the input power injected. For more detail, readers can refer to this paper[11]. For the measurements, as dictated by the protocol, 20 repetitions of 1 s each were acquired and summed up. Moreover, before computing the responsivity value the background noise was removed from the recorded curves.

2.3 nEUROPt protocol

The nEUROPt protocol was conceived to objectively assess the capability of a diffuse optics instrument to detect, localize and quantify the absorption changes into a homogeneous diffuse medium. In the nEUROPt protocol, several tests have been devised to test the sensitivity, spatial resolution, and quantification but, in this work, we limit our study to the first aspect (i.e., capability to detect an absorption change). To this extent, the nEUROPt protocol adopted two tests: the contrast (C) and the contrast to noise ratio (CNR). The former is defined as the relative change into the number of photons detected when an optical perturbation is present in the medium. More in detail, as expressed by Eq. (1), the contrast is the difference between the number of counts detected in the "homogenous case" (N_0, i.e., medium without any optical inhomogeneity) and the number of photons detected in the so-called "perturbated or heterogeneous state" (N, i.e., with the perturbation inside the medium), divided by the number of homogeneous counts.

$$C = (N_0\text{-}N)/N_0 \tag{1}$$

On the other hand, the CNR is an index of the robustness of the contrast with respect to the fluctuation of the measurements (in the homogeneous case), as enlightened by Eq. 2

$$CNR = (N_0\text{-}N)/\ \sigma(N_0) \tag{2}$$

where $\sigma(N_0)$ is the standard deviation over the repetitions of the number of counts in the homogeneous case. The theoretical limit for CNR is 1, below that value any contrast is not significant since it cannot be distinguished from measurements' fluctuations.

Both C and CNR can be computed within gates (i.e., time-windows selecting a portion of the DTOF) whose position is always referred to the peak of Instrument Response Function (IRF)[11]. The gate width was set to 1000 and 500 ps, in measurements and simulations respectively.

2.4 MEDPHOT protocol

The MEDPHOT protocol is meant to quantify the capability of a DO system to properly recover the optical properties of homogenous samples[16]. Among the several tests proposed in the protocol, we adopted the linearity in the retrieval of both μ_a and μ_s' that shows the dependence of the optical parameters against their conventionally true values.

For what concerns the data analysis, after removing the background noise, DTOFs were fitted using the analytical model of photon transportation in diffusive semi-infinite media[22] to recover the optical coefficients. To take into account the

non-idealities due to the finite response of the system, we convolved the theoretical response with the IRF before fitting the data. When the χ^2 (i.e., the index of the quality of the fitting operation) is minimized, the fitting algorithm approaches convergence[23].

2.5 Simulations

Simulations have been used to study the possibility to work well-beyond the single-photon statistics thus overcoming the bottleneck in the maximum number of detected photons for detector with very large responsivity, as the one described in Par. 2.1.

We simulate DTOFs acquired in reflectance geometry using the radiative transfer equation under the diffusion approximation. As sample geometry, we consider semi-infinite medium either homogenous or embedding localized perturbation[22]. To evaluate the performance of a cutting-edge DO detector, we convolved the theoretical DTOF with a typical IRF of a SiPM-based TD system[19]

We generate two distinct sets of data. The first is meant to allow MEDPHOT protocol analysis and it considers a set of 8 phantoms: 4 with μ_a = 0.1, 0.2, 0.3, 0.4 cm^{-1} at fixed μ_s' = 10 cm^{-1} and 4 with μ_s'= 5, 10, 15, 20 cm^{-1} at a fixed μ_a = 0.1 cm^{-1}. The second generated set of data is meant to apply the nEUROPt protocol analysis and, in this case, we consider a bulk homogenous phantom with μ_a = 0.1 cm^{-1} and μ_s' = 10 cm^{-1} embedding a localized absorption perturbation (volume: 1 cm^3) with $\Delta\mu_a$ of 0.17 cm^{-1} placed at half of the source-detector separation (SDS) and at a distance of 1.5 cm from the surface. Both datasets have been simulated considering a 40 MHz laser excitation rate, a time-correlated single-photon counting board with channel width of 5 ps, a SDS of 3 cm and an elliptical collection area of 1 x 1.78 cm^2 (with the major axis orthogonal to the SDS). We generated curves up to 12 ns and with a DCR of 100 kcps. To add to these theoretical DTOFs the classical pile-up distortion (i.e., distortion due to the inability of the timing hardware to process more than one photon per excitation cycle), we use a MATLAB code based on random Poisson launches that distort the input probability distribution, simulating the physical process currently occurring in real measurements (also adding in this way a realistic Poisson noise). As correction procedure we use a simple, yet effective algorithm proposed by Coates, where there is no need to rely on previous knowledge of the input curve[14].

We considered 3 different saturated CRs (values after the pile-up distortion): 1.24, 25.28 and 39.86 Mcps (equivalent to after-correction values of 1.26, 40 and 225 Mcps).

3. RESULTS AND DISCUSSION

3.1 Experimental measurements

Figure 1 reports the spectral responsivity computed for the 1 cm^2 module. In the same graph, the responsivity for the cutting-edge research technology (3 mm^2 probe-hosted SiPM working in high throughput[13]), state-of-the-art research technology (1 mm^2 SiPM probe-hosted SiPM[24]) and state-of-the-art clinical instrument[25] (based on photomultiplier tubes) are reported for comparison. The proposed detector shows an improvement of almost 1 decade with respect to the cutting-edge research technology, while the improvement with respect to the system presented in Ref.[24] is of a factor 30 or 80 (depending on the wavelength). An even larger increase (> 100) in the light harvesting capability can be appreciated if the state-of-the--art clinical system is considered[25].
Thanks to the very large responsivity, a SDS of 11 cm was used to increase the sensitivity to late photons. The results obtained in terms of contrast and CNR are reported in Figure 2 (respectively left and right graph). As explained in Par. 2.3, the theoretical limit for contrast visibility is CNR≥1 thus from contrast graph (left plot of Figure 2) all points which were not fulfilling this condition were removed. Looking at the contrast graph, it is possible to see that increasing the gate delay there is an improvement in the visibility of deep perturbation, as predicted by theory. Considering as a minimum detectable contrast the value of 0.01 (i.e., conventionally assumed as the biological variability in living tissues), we can distinguish a perturbation buried up to 38.5 mm.

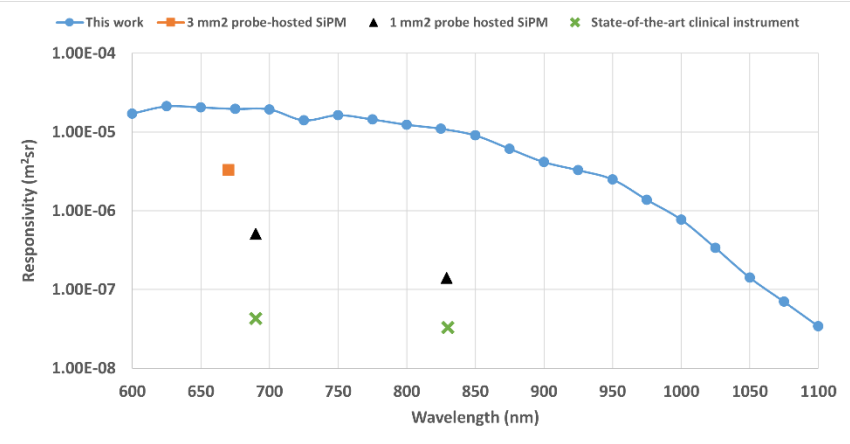

Figure 1. Responsivity of the 1 cm^2 SiPM module, compared to other cutting-edge instruments (e.g., 3 mm^2 and 1 mm^2 probe hosted SiPM, respectively Ref[13,24]) and state-of-the-art clinical system[25].

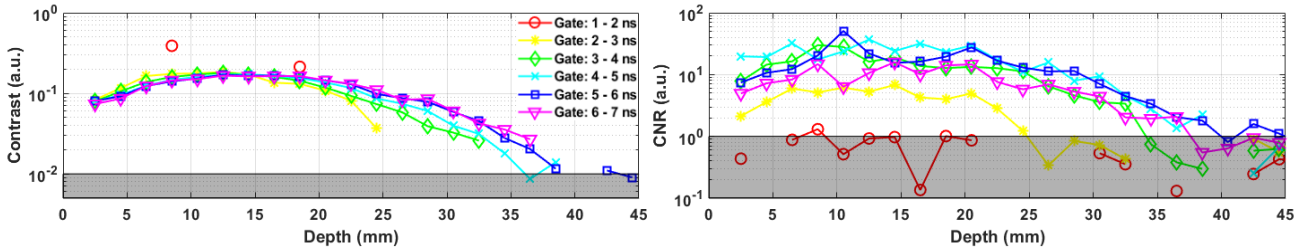

Figure 2. Contrast (left graph) and CNR (right graph) computed for different gates (colors). The gray shadowed regions represent values which are considered not significative (i.e., contrast lower than 0.01 and CNR lower than 1).

Eventually, we challenged our detector with the linearity tests dictated by the MEDPHOT protocol (conducted in trasmittance geometry), as explained in Par. 2.4. The linearity test in the retrieval of the absorption coefficient (for all the scattering series, different colors) is reported in the left panel of Figure 3. Looking at the graph, the system is capable of properly recovering linear variation of the absorption coefficient over a wide range of optical properties. Moreover, also the accuracy in the retrieved value (i.e., closeness of the values to the dotted line) is good, with slight deviations from the expected value only for very high absorption values (0.46 cm^{-1}).

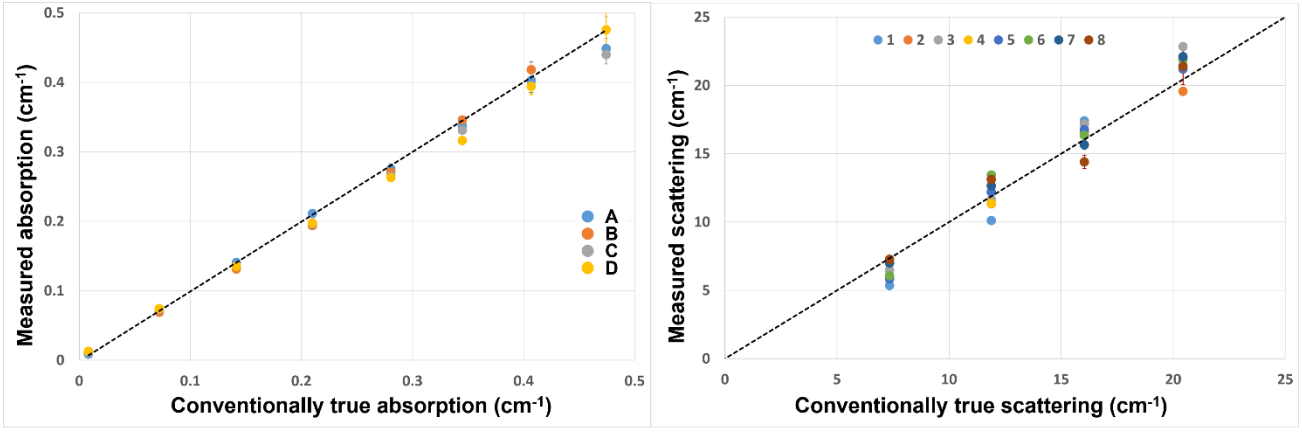

Figure 3. Linearity in the retrieval of absorption coefficient for several scattering series (left graph) and linearity in the retrieval of the scattering coefficient for all the eight absorption phantom series (right graph). In both graphs, the dashed line represents the expected values.

For what concerns the linearity in the retrieval of the scattering coefficient (see the right graph of Figure 3), the system is capable to retrieve linear variation in the scattering coefficient for the whole absorption phantom series (different colors). On the other hand, for what concerns the accuracy in the retrieval of the scattering coefficient, a not-negligible spreading of the recovered value with respect to the expected one is present thus showing a limited accuracy. However, the lower accuracy in the retrieval of the scattering coefficient with respect to the absorption one is a well-known criticality of the time-domain diffuse optical systems[16]. For both cases, the error bars (i.e., standard deviation over the 20 repetitions of the measurements) are almost negligible thus enlightening the stability of the system in the retrieval of the optical properties.

3.2 Simulations

Figure 4 shows linearity in retrieving μ_a (left) and μ_s' (right) at 3 different CRs. In particular, it reports the retrieved μ_a (μ_s') as a function of the conventionally true μ_a (μ_s') at the fixed μ_s' (μ_a).
For the absorption linearity before pile-up correction (solid lines), the in-statistic CR (i.e., 1.24 Mcps, blue round marker) shows a small underestimation of the retrieved μ_a (slope < 1). On the opposite, all the other cases (25.28 and 39.86 Mcps, red asterisks and green crosses, respectively) show a general overestimation of recorded μ_a, particularly, exaggerated for the extreme CR, where the slope is far from unity (see inset in the left graph of Figure 4). Concerning the after-correction curves there is no improvements for 1.24 Mcps, as expected, since the system is working within single-photon statistics thus no relevant pile-up effect is present to be corrected. On the other hands, 25.28 and 39.86 Mcps show good linearity (slope close to 1, i.e., close to the solid black line), performing better than in-statistic working regime.
On the other hand, for the scattering linearity, both 1.24 and 25.28 Mcps reports an underestimation of the retrieved μ_s' (slope < 1) while 39.86 Mcps overestimates the retrieved optical property. For what concern the situation after correction, still, no improvements are noticeable for the in-statistic case, as expected. While for 25.28 and 39.86 Mcps there is good linearity, with slopes close to unity.
Figure 5 reports C (left) and CNR (right) as a function of the CR, evaluated in the gate that maximizes the C at each CR. Both before (blue line) and after correction (red line) values are shown. The gray shaded area on right side plot highlights the region where C<1% (as in Figure 2). For C before correction, we can observe that as the CR increases, the maximum C decreases. This is an expected behavior, since the pile-up effect reduces the amount of observed photons in the DTOF's tail as the CR grows. As a result, the homogeneous curve is pushed further towards the heterogeneous curve (which is less affected by pile-up due to the lower number of counts), and the difference in the number of counts between the perturbed and unperturbed states is decreased, reducing C. Furthermore, at 39.86 Mcps the C is lower than 0.01, thus preventing the detection of the perturbation. This problem is solved if the correction algorithm is applied. Indeed, in terms of after-correction values, the Coates algorithm has an effect on 25.28 and 39.86 Mcps, while the 1.24 Mcps remains unchanged, as predicted. In particular, the highest C possible is restored in all cases (now the perturbation is visible at 39.86 Mcps), showing that, according to the theory, C should not be affected by the number of photons detected[26].

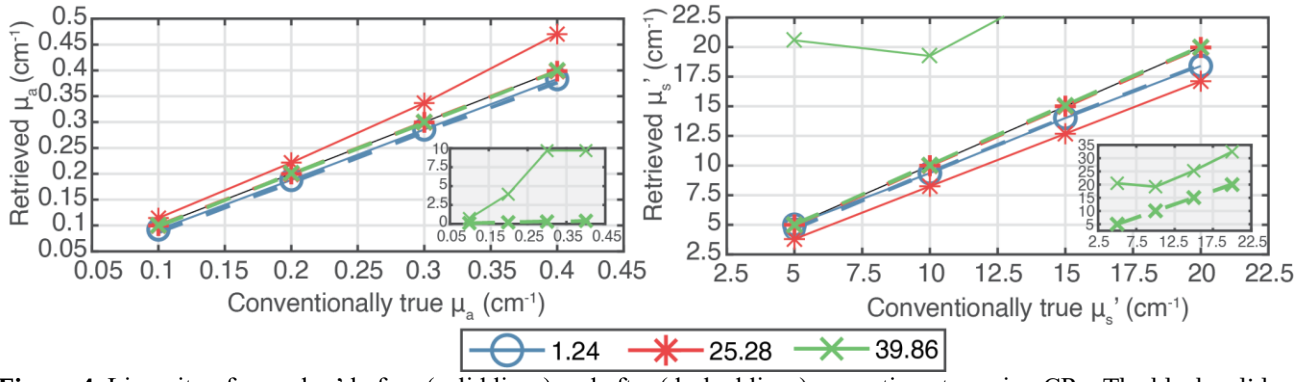

Figure 4. Linearity of μ_a and μ_s' before (solid lines) and after (dashed lines) correction at varying CRs. The black solid line represents the expected values.

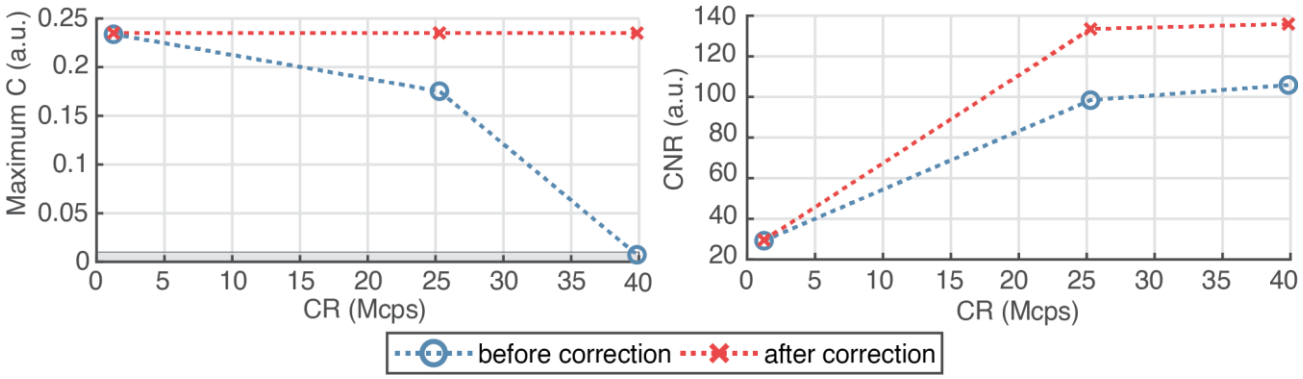

Figure 5. C (left) and CNR (right) computed in the gate where C is maximized, as a function of the CR. Blue line refers to the before-correction values, while red line refers to the after-correction one. In the right plot, the grey region indicates where C < 0.01.

The CNR before correction, on the other hand, increases with the CR. This is justified by the fact that the number of detected photons is growing, and that, even if the pile-up effect distorts curves, the overall signal to noise ratio is increasing as well. In terms of the after-correction CNR, Coates method has obviously no effect on the in-statistic scenario, while for 25.28 Mcps and 39.86 Mcps, it is improved above the before-correction case. As a consequence, the C becomes more resistant in terms of noise fluctuations, boosting the reliability of its final result.

4. CONCLUSIONS AND FUTURE PERSPECTIVES

In this work we present the largest area microelectronic single-photon detector ever validated for TD-DO, featuring an area of about 1 cm^2. The detector shows a responsivity which is almost 1 order of magnitude higher than the best-in class cutting-edge research technology system[13]. Thanks to the high light harvesting capability, it is possible to enlarge significantly the SDS thus improving the sensitivity to a deep perturbation. To verify this, we performed the nEUROPt sensitivity tests with SDS of 11 cm demonstrating a maximum penetration depth of 38.5 mm, which is in line with best state-of-the-art system[17,27]. We also challenged our detector with the linearity test of the MEDPHOT protocol achieving good results both in terms of linearity and also in accuracy (which is good for absorption coefficient and sufficient for the scattering one).

Considering the very large responsivity of the detector, we started devising a new operational regime above the single-photons statistics which will allow to exploit the whole number of detected photons at short SDS. To this extent, we made simulations at three different count-rate (in-statistics, above and well-above statistics) and we used the simulated data to perform the same tests of nEUROPt and MEDPHOT protocols adopted for the measurements. Providing that a suitable algorithm is applied (such as the one proposed by Coates[14]), the use of a count-rate well above single-photon statistics improves the visibility of an absorption perturbation in-depth (improvement in CNR) while keeping good results in terms of linearity and accuracy of absorption and scattering coefficient retrieval for a homogeneous medium. Such an in-silico work allows us to open a new horizon for TD-DO measurements paving the way to new applications as, for example, the study of deep layered structures like the chest for lung monitoring applications. Moreover, the possibility to work at a very high count-rate opens up new approaches to measurements: on one side, fixing the overall number of counts, it could be possible in future works to decrease the measurement time of order of magnitude while, on the other side, keeping the measurement time constant, it could be possible to improve the penetration in the detection of deep localized perturbations.

We are currently working on the experimental implementation of such well above single-photon statistics regime and tests both on-phantom and *in-vivo* will be carried on in the next months.

ACKNOWLEDGEMENTS

This research has received funding from the ATTRACT project funded by EU under grant agreement no 777222.

REFERENCES

[1] Chance, B., [Photon Migration in Tissues], Plenum Press, New York (1989).

[2] Pifferi, A., Contini, D., Dalla Mora, A., Farina, A., Spinelli, L. and Torricelli, A., "New frontiers in time-domain diffuse optics, a review," J. Biomed. Opt. **21**(9), 091310 (2016).

[3] Dalla Mora, A., Contini, D., Arridge, S., Martelli, F., Tosi, A., Boso, G., Farina, A., Durduran, T., Martinenghi, E., Torricelli, A. and Pifferi, A., "Towards next-generation time-domain diffuse optics for extreme depth penetration and sensitivity," Biomed. Opt. Express **6**(5), 1749–1760 (2015).

[4] Di Sieno, L., Nissinen, J., Hallman, L., Martinenghi, E., Contini, D., Pifferi, A., Kostamovaara, J. and Dalla Mora, A., "Miniaturized pulsed laser source for time-domain diffuse optics routes to wearable devices," J. Biomed. Opt. **22**(8), 085004 (2017).

[5] Saha, S., Lu, Y., Weyers, S., Sawan, M. and Lesage, F., "Compact Fast Optode-Based Probe for Single-Photon Counting Applications," IEEE Photonics Technol. Lett. **30**(17), 1515–1518 (2018).

[6] Ban, H. Y., Barrett, G. M., Borisevich, A., Chaturvedi, A., Dahle, J. L., Dehghani, H., DoValle, B., Dubois, J., Field, R. M., Gopalakrishnan, V., Gundran, A., Henninger, M., Ho, W. C., Hughes, H. D., Jin, R., Kates-Harbeck, J., Landy, T., Lara, A. H., Leggiero, M., et al., "Kernel Flow: a high channel count scalable TD-fNIRS system," Integr. Sensors Biol. Neural Sens. **11663**, H. Mohseni, Ed., 24–42, SPIE (2021).

[7] Dalla Mora, A., Di Sieno, L., Behera, A., Taroni, P., Contini, D., Torricelli, A. and Pifferi, A., "The SiPM revolution in time-domain diffuse optics," Nucl. Instruments Methods Phys. Res. Sect. A Accel. Spectrometers, Detect. Assoc. Equip. **978**, 164411 (2020).

[8] Martinenghi, E., Di Sieno, L., Contini, D., Sanzaro, M., Pifferi, A. and Dalla Mora, A., "Time-resolved single-photon detection module based on silicon photomultiplier: A novel building block for time-correlated measurement systems," Rev. Sci. Instrum. **87**(7) (2016).

[9] Ferocino, E., Martinenghi, E., Dalla Mora, A., Pifferi, A., Cubeddu, R. and Taroni, P., "High throughput detection chain for time domain optical mammography," Biomed. Opt. Express **9**(2), 755–770 (2018).

[10] Di Sieno, L., Behera, A., Rohilla, S., Ferocino, E., Contini, D., Torricelli, A., Krämer, B., Koberling, F., Pifferi, A. and Dalla Mora, A., "Probe-hosted large area silicon photomultiplier and high-throughput timing electronics for enhanced performance time-domain functional near-infrared spectroscopy," Biomed. Opt. Express **11**(11), 6389–6412 (2020).

[11] Wabnitz, H., Taubert, D. R., Mazurenka, M., Steinkellner, O., Jelzow, A., Macdonald, R., Milej, D., Sawosz, P., Kacprzak, M., Liebert, A., Cooper, R., Hebden, J., Pifferi, A., Farina, A., Bargigia, I., Contini, D., Caffini, M., Zucchelli, L., Spinelli, L., et al., "Performance assessment of time-domain optical brain imagers, part 1: basic instrumental performance protocol," J. Biomed. Opt. **19**(8), 86010 (2014).

[12] Becker, W., [The bh TCSPC handbook 6th edition] (2014).

[13] Di Sieno, L., Behera, A., Rohilla, S., Ferocino, E., Contini, D., Torricelli, A., Krämer, B., Koberling, F., Pifferi, A. and Dalla Mora, A., "Probe-hosted large area silicon photomultiplier and high-throughput timing electronics for enhanced performance time-domain functional near-infrared spectroscopy," Biomed. Opt. Express **11**(11), 6389 (2020).

[14] Coates, P. B., "The correction for photon 'pile-up' in the measurement of radiative lifetimes," J. Phys. E. **1**(8), 878–879 (1968).

[15] Wabnitz, H., Jelzow, A., Mazurenka, M., Steinkellner, O., Macdonald, R., Milej, D., Zolek, N., Kacprzak, M., Sawosz, P., Maniewski, R., Liebert, A., Magazov, S., Hebden, J., Martelli, F., Di Ninni, P., Zaccanti, G., Torricelli, A., Contini, D., Re, R., et al., "Performance assessment of time-domain optical brain imagers, part 2: nEUROPt protocol," J. Biomed. Opt. **19**(8), 86012 (2014).

[16] Pifferi, A., Torricelli, A., Bassi, A., Taroni, P., Cubeddu, R., Wabnitz, H., Grosenick, D., Möller, M., Macdonald, R., Swartling, J., Svensson, T., Andersson-Engels, S., van Veen, R. L. P., Sterenborg, H. J. C. M., Tualle, J.-M., Nghiem, H. L., Avrillier, S., Whelan, M. and Stamm, H., "Performance assessment of photon migration instruments: the MEDPHOT protocol.," Appl. Opt. **44**(11), 2104–2114 (2005).

[17] Behera, A., Acerbi, F., Gola, A., Dalla Mora, A. and Di Sieno, L., "Performance of 6x6 mm^2 SiPM module for time-domain diffuse optics," IEEE J. Sel. Top. Quantum Electron., 1–1 (2021).

[18] Acerbi, F., Behera, A., Dalla Mora, A., Di Sieno, L. and Gola, A., "Single-Photon Detection Module Based on Large-Area Silicon Photomultipliers for Time-Domain Diffuse Optics," Instruments **5**(2) (2021).

[19] Konugolu Venkata Sekar, S., Dalla Mora, A., Bargigia, I., Martinenghi, E., Lindner, C., Farzam, P., Pagliazzi,

M., Durduran, T., Taroni, P., Pifferi, A. and Farina, A., "Broadband (600-1350 nm) Time-Resolved Diffuse Optical Spectrometer for Clinical Use," IEEE J. Sel. Top. Quantum Electron. **22**(3), 7100609 (2016).
[20] Spinelli, L., Martelli, F., Farina, A., Pifferi, A., Torricelli, A., Cubeddu, R. and Zaccanti, G., "Calibration of scattering and absorption properties of a liquid diffusive medium at NIR wavelengths. Time-resolved method," Opt. Express **15**(11), 6589–6604 (2007).
[21] Martelli, F., Di Ninni, P., Zaccanti, G., Contini, D., Spinelli, L., Torricelli, A., Cubeddu, R., Wabnitz, H., Mazurenka, M., Macdonald, R. and others., "Phantoms for diffuse optical imaging based on totally absorbing objects, part 2: experimental implementation," J. Biomed. Opt. **19**(7), 76011 (2014).
[22] Martelli, F., Del Bianco, S., Ismaelli, A. and Zaccanti, G., [Light propagation through biological tissue and other diffusive media: Theory, solutions, and software], SPIE (2009).
[23] Press, W. H., Teukolsky, S. A., Vetterling, W. T. and Flannery, B. P., "Numerical recipes in C," Cambridge Univ. Press **1**, 3 (1988).
[24] Re, R., Martinenghi, E., Dalla Mora, A., Contini, D., Pifferi, A. and Torricelli, A., "Probe-hosted silicon photomultipliers for time-domain functional near-infrared spectroscopy: phantom and in vivo tests," Neurophotonics **3**(4), 045004 (2016).
[25] Re, R., Contini, D., Turola, M., Spinelli, L., Zucchelli, L., Caffini, M., Cubeddu, R. and Torricelli, A., "Multi-channel medical device for time domain functional near infrared spectroscopy based on wavelength space multiplexing," Biomed. Opt. Express **4**(10), 2231–2246 (2013).
[26] Behera, A., Di Sieno, L., Pifferi, A., Martelli, F. and Dalla Mora, A., "Instrumental, optical and geometrical parameters affecting time-gated diffuse optical measurements: a systematic study," Biomed. Opt. Express **9**(11), 5524–5542 (2018).
[27] Di Sieno, L., Ferocino, E., Conca, E., Sesta, V., Buttafava, M., Villa, F., Zappa, F., Contini, D., Torricelli, A., Taroni, P., Tosi, A., Pifferi, A. and Dalla Mora, A., "Time-domain diffuse optics with 8.6 mm2 fast-gated SiPM for extreme light harvesting," Opt. Lett. **46**(2), 424–427 (2021).